Hindawi
Quantum Engineering
Volume 2024, Article ID 9972747, 8 pages
https://doi.org/10.1155/2024/9972747

Research Article

The Detection of Explosive Cyclotrimethylenetrinitramine (RDX) Using Optical Microcavity

Yao Shen,[1] Kai Wang,[2] Bai-En Guo,[1] and Min Wang[3]

[1]*School of Criminal Investigation, People's Public Security University of China, Beijing 100038, China*
[2]*Department of Physics, Beijing University of Posts and Telecommunications, Beijing 100876, China*
[3]*Beijing Academy of Quantum Information Sciences, Beijing 100193, China*

Correspondence should be addressed to Min Wang; wangmin@baqis.ac.cn

Received 7 February 2024; Revised 24 February 2024; Accepted 1 March 2024; Published 9 March 2024

Academic Editor: YuBo Sheng

Optical microcavity, which is based on light-matter interaction, has the advantage of high sensitivity as a sensor. It has been widely used in the security, medicine, and environment fields these years. Detection of atoms and molecules at the nanoscale is one of the practical usages of optical microcavity. In this paper, we focus on a ultra-high-quality factor optical microcavity of whispering gallery mode (WGM) to detect the explosive of cyclotrimethylenetrinitramine (RDX). To demonstrate the high sensitivity of the method, we detect the solution at different concentrations. Different types of optical microcavities are suitable for the detection of different matters. Considering the effects of the results and the simplicity of operation, we use silica microspheres chiefly. This is the first time to detect the explosive using highly sensitive optical microcavity. The detection of pure explosives will be helpful for establishing the database of the explosives.

1. Introduction

Analogous to the principle of tuning forks, optical microcavity could confine light to a certain volume to create resonant recirculation. The principle of optical microcavity is based on the light-matter interaction. Because of the total reflection, light is restricted in the optical microcavity that has a symmetrical configuration. The light in the microcavity couples with the light in the fiber. Under certain conditions, the intensity of light will be strengthened. Optical microcavity has its own resonant mode because of its special configuration. When molecules adhere to the surface of a microcavity, the change in system configuration leads to the change of the resonant mode. Generally speaking, these changes in the form of frequencies are easy to observe. The ideal condition is that the resonator can be indefinite or lossless, so the resonant frequencies are precise. The quality of optical microcavity is measured by Q factor [1–3]. Q factor and the microcavity volume are the main parameters of optical microcavity [4–6]. According to the confinement style, optical microcavities could be divided into three categories: Fabry–Perot microcavity [7–10], photonic crystal microcavity [11], and whispering gallery mode (WGM) microcavity [12–14]. Fabry–Perot microcavities [7, 8] have two mirrors to feedback light. The emitter of micropost (quantum dot for example) triggers single photon emission via the Purcell effect. The high Q and small volume could reach $Q = 2000$ and $V = 5\ (\lambda/n)^3$, where n is the refraction index. Instead of the center of mass motion, the ultracold atom in a strong couple system interacted with the vacuum cavity mode has a ultrahigh Q: $F = 4.8 \times 10^5$ (F is opposed to Q) with $V = 1.69 \times 10^3 \mu m^3$ [9, 10]. Photonic crystal microcavities [11] have a hole drilled in the middle of the structure, and a neutral atom located in the hole forms the donor mode geometries with $Q = 1.3 \times 10^4$. High Q WGM microcavities include microdiscs [15–18] with $Q = 12000$ and add/drop filters (semiconductor or polymer) [19, 20] with $Q = 7000$ or $Q = 1.3 \times 10^5$ respectively. Silica or quartz microsphere [21] and microdisk type [5, 22] WGMs are ultrahigh Q microcavities with $Q = 8 \times 10^9$ and $Q = 10^8$. Lights are reflected continuously in spherical and toroidal structures. Because of the high sensitivities and

practicabilities of nanoparticle detection, we focus on microsphere WGMs.

WGM optical microcavity is a highly potential technology in forensic science. It has many advantages. First, the price is much cheaper than other traditional instruments such as a gas chromatograph spectrometer. Second, some detection technologies search certain ligand rather than the whole molecule [23, 24]. This will cause the high error detection rate. Optical microcavity detects the molecule, so this technology has more accuracy [25, 26]. Third, traditional instruments detect either liquid phase or gas phase (only one phase), and the samplings are all liquid phases (gas phase needs to heat the liquid sampling). This is a limitation. The sample injection of optical microcavity can be liquid phase or gas phase which means there is no need to prepare the gas sample into solution. The gas sample can be detected by injecting the gas directly into microcavity [27]. Fourth, as long as there is a molecule attached to the microcavity, the response to the change in frequencies is obvious [28, 29]. Optical microcavity has ultrahigh sensitivity which could reach nanoscale [30, 31]. Fifth, it is easy to operate and really takes a short time to get the result. When the sample is injected into or onto optical microcavity (depends on the configuration of microcavity), the results will be immediate and obvious. This is a dynamic real-time processing. All of these advantages show the necessity and potential of this technology application in forensic science. In this paper, we show the viability of this detection technology in forensic science, so we use the WGM silica microsphere cavity to detect RDX as an example.

This paper is organized as follows: In Section II, we introduce the method and apparatus used in our experiment. In section III, we give the results of detection of solutions of different concentrations and compare them with the results of solution with no determinant. Finally, in section IV, the main results are concluded and further work is discussed.

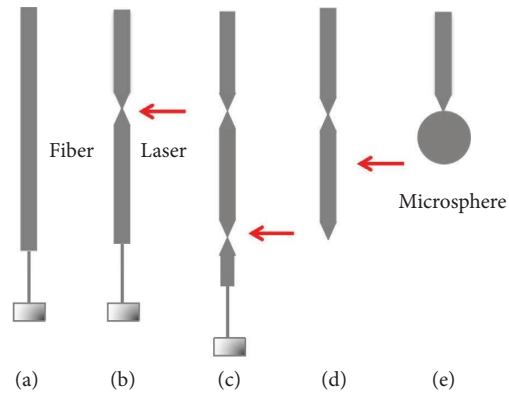

Figure 1: The manufacturing process of microsphere microcavity. Schematic of the silica or quartz microsphere type whispering gallery mode (WGM) microcavity.

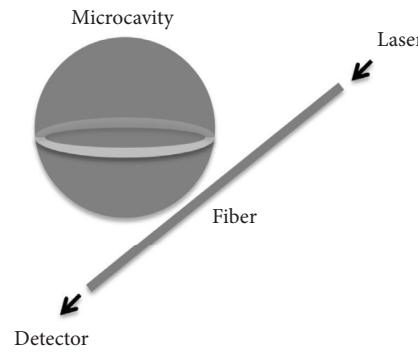

Figure 2: Schematic of the silica or quartz microsphere type whispering gallery mode (WGM) microcavity. The coupling method we use is critical coupling, and there is a small gap between the optical fiber and the microcavity, the fiber is not placed on the periphery of the sphere.

2. Method and Apparatus

In the first step, we fabricate the microsphere cavities with diameter 64 μm using CO_2 laser device of SYNRAD 48-2KAM-AP (see Figure 1). First of all, we get rid of the protective layer of the optical fiber (taper fiber), clean it with alcohol, and weight an object at the end of the fiber vertically. Lately, the fiber has been heated by a low-power CO_2 laser. The heat melts the fiber but it doesn't break it. Next, we cut off the weight at the appropriate position of the fiber using a high-power CO_2 laser. After that, the rest of the fiber is heated to reflux. Finally, we get a microsphere cavity.

In the second step, we dip the microsphere cavities into a diluted solution or drip the solution drop onto the microsphere cavities. The laser propagates along the optical fiber and interacts with the molecules suspended in the solution (see Figure 2). The molecules suspended in the solution change the vibration mode of the microsphere cavity. These changes affect the responses on the oscilloscopes. The laser device is the New Focus Tunable Laser Controller TLB-6700. The wave range from 1540 nm to 1550 nm. The power of the laser we used is 2 mW. The signal generator used in the experiment is Tektronix AFG3022C and the oscilloscope is Tektronix MDO3104. We use a triangular wave with frequency 50 Hz and amplitude $2V$ ($-1V \sim 1V$). The standard solution is made of the explosive of Cyclotrimethylenetrinitramine (RDX) in acetone of concentration of 1000 ppm, and it is diluted by alcoholic.

3. The Results and Analysis of Diluted Standard Solution of Different Concentration

The microsphere cavities of whispering gallery mode (WGM) could be used to detect very few molecules and small microparticles. On the contrary, too many molecules and small microparticles would reduce the Q factor and thus make the results unreasonable. According to this, we dilute the standard solution into three concentrations. The ratios of the standard solution and the alcoholic solution are 1 : 1, 1 : 2, and 1 : 3. And we compare the 1 : 2 result with acetone solution which is diluted by equivalent alcohol. All experiments with different concentrations are repeated three

times, and the results are similar. According to the standard deviations, we chose the figures of the best results here to demonstrate.

3.1. The Result of Ratio 1 : 1 (Standard Solution: Alcoholic Solution). We dip the microsphere cavities in the diluted solution of ratio 1 : 1. The vibration mode of the microsphere cavity is changed because of the existence of the molecules suspended in the solution (see Figures 3 and 4). Figure 3 shows the original mode of the microsphere cavity. In this case, the central frequencies of two modes are $\omega_1 = 1218.74564\,\text{THz}$ and $\omega_2 = 1218.75304\,\text{THz}$. The widths of them are $\Delta\omega_{1h} = 7.89303 \times 10^{-5}\,\text{THz}$ and $\Delta\omega_{2h} = 1.69600 \times 10^{-4}\,\text{THz}$. The vertical coordinate is the normalized transmission spectrum. In Figure 4, after we dip the microsphere cavities into diluted solution, both of the two original modes move towards left and split into two parts. The first frequency ω_1 turns to $\omega_{11} = 1218.73921\,\text{THz}$ and $\omega_{12} = 1218.73952\,\text{THz}$. The widths are $\Delta\omega_{11h} = 1.77393 \times 10^{-4}\,\text{THz}$ and $\Delta\omega_{12h} = 1.50420 \times 10^{-4}\,\text{THz}$, respectively. The second frequency ω_2 becomes $\omega_{21} = 1218.74438\,\text{THz}$ and $\omega_{22} = 1218.74473\,\text{THz}$. The widths of them are $\Delta\omega_{21h} = 6.41991 \times 10^{-5}\,\text{THz}$ and $\Delta\omega_{22h} = 6.20527 \times 10^{-5}\,\text{THz}$. The split frequency of the first mode is $\omega_{12} - \omega_{11} = 0.31\,\text{GHz}$, and that of the second mode is $\omega_{22} - \omega_{21} = 0.35\,\text{GHz}$. The RDX molecules suspended in the solution adhere to the microsphere cavity cause the split. The losses in the experiment are divided into intrinsic losses and coupling losses. We summarize the result in the Table 1.

3.2. The Result of Ratio 1 : 2 (Standard Solution: Alcoholic Solution). As per the procedure we mentioned above, we dilute the standard solution with alcohol of the ratio 1 : 2 this time. The frequency of the original mode is $\omega_1 = 1223.64186\,\text{THz}$. Its width is $\Delta\omega_{1h} = 5.79740 \times 10^{-5}\,\text{THz}$. The target molecules in the diluted solution result in the left move and the split of the original mode. Two frequencies of new modes are $\omega_{11} = 1223.63137\,\text{THz}$ and $\omega_{12} = 1223.63160\,\text{THz}$. Their widths are $\Delta\omega_{11h} = 2.93266 \times 10^{-4}\,\text{THz}$ and $\Delta\omega_{12h} = 2.52107 \times 10^{-4}\,\text{THz}$. The split frequency becomes $\omega_{12} - \omega_{11} = 0.23\text{GHz}$ (see Figures 5 and 6). The result is summarized in Table 2.

3.3. The Result of Ratio 1 : 3 (Standard Solution: Alcoholic Solution). We continue diluting the standard solution with alcohol in the ratio 1: 3. In the beginning, the frequency of the vibration mode of the cavity is $\omega_1 = 1223.13682\,\text{THz}$ with width $\Delta\omega_{1h} = 5.71579 \times 10^{-5}\,\text{THz}$. The target molecules are adsorbed to the external surface of the cavity which gives us two smaller frequencies of new modes $\omega_{11} = 1223.13536\,\text{THz}$ and $\omega_{12} = 1223.13556\,\text{THz}$. Their widths are $\Delta\omega_{11h} = 2.79271 \times 10^{-4}\,\text{THz}$ and $\Delta\omega_{12h} = 3.09351 \times 10^{-4}\,\text{THz}$. The split frequency turns to be $\omega_{12} - \omega_{11} = 0.20\,\text{GHz}$ (see Figures 7 and 8). From the results above, we can conclude, the lower the concentration is the smaller the split frequency becomes (see Table 3).

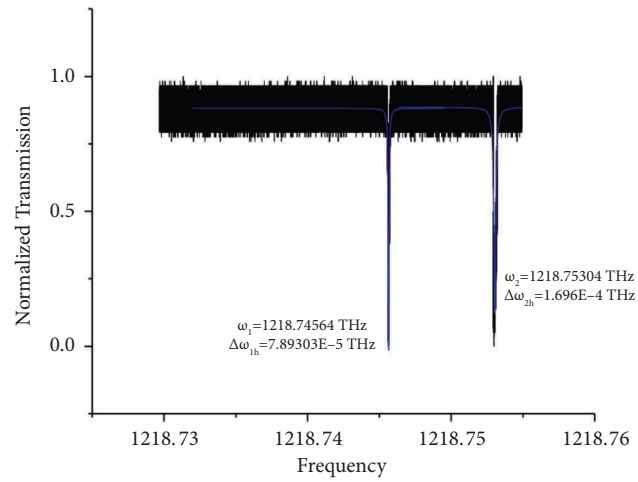

Figure 3: The frequency distribution of microsphere cavity with no solution. The blue line shows two peaks of original vibration modes.

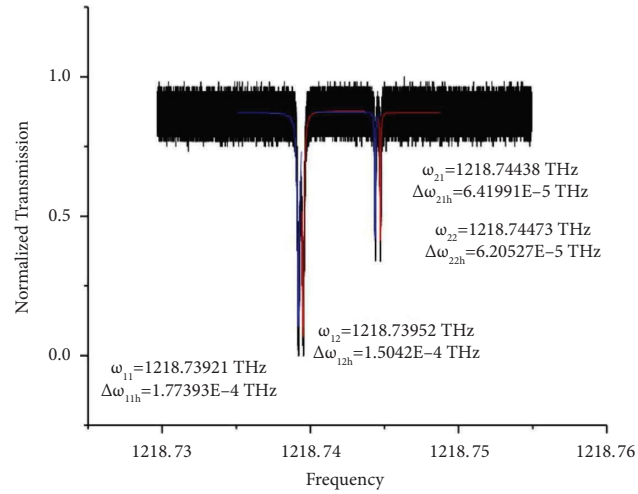

Figure 4: The frequency distribution of microsphere cavity with diluted solution. The ratio of the standard solution and the alcoholic solution is 1 : 1. The blue line and red line represent the split of two original frequencies.

3.4. The Result of the Solution with No Determinant (Acetone Solution: Alcoholic Solution = 1 : 2). In the end, we discuss the solution of pure acetone with no RDX molecules and compare it with the result above. Because of the absence of target molecules, the mode of microcavity does not split. The peak of the mode frequency only moves from $\omega = 1223.94771\,\text{THz}$ to another position $1223.94444\,\text{THz}$ with the broadening of the width from $\Delta\omega = 1.38211 \times 10^{-4}\,\text{THz}$ to $3.40387 \times 10^{-4}\,\text{THz}$. The change of the frequency reads 3.27 GHz (see Figures 9 and 10). Whether there exist RDX molecules in the solution or not, the peaks of the diluted solution change to smaller values. Because the solution with no RDX molecules changes the mode volume (the mode distribution) of the microcavity. When the RDX molecules adhere to the microcavity, besides the shift of the frequency peaks, the peaks split and broaden simultaneously.

Table 1: The result of ratio 1 : 1 (standard solution: alcoholic solution).

Original mode	$\omega_1 = 1218.74564\,\text{THz}$
Original mode	$\omega_2 = 1218.75304\,\text{THz}$
Widths	$\Delta\omega_{1h} = 7.89303 \times 10^{-5}\,\text{THz}$
Widths	$\Delta\omega_{2h} = 1.69600 \times 10^{-4}\,\text{THz}$
RDX mode	$\omega_{11} = 1218.73921\,\text{THz}$, $\omega_{12} = 1218.73952\,\text{THz}$
RDX mode	$\omega_{21} = 1218.74438\,\text{THz}$, $\omega_{22} = 1218.74473\,\text{THz}$
Widths	$\Delta\omega_{11h} = 1.77393 \times 10^{-4}\,\text{THz}$, $\Delta\omega_{12h} = 1.50420 \times 10^{-4}\,\text{THz}$
Widths	$\Delta\omega_{21h} = 6.41991 \times 10^{-5}\,\text{THz}$, $\Delta\omega_{22h} = 6.20527 \times 10^{-5}\,\text{THz}$
Split frequency	$\omega_{12} - \omega_{11} = 0.31\,\text{GHz}$
Split frequency	$\omega_{22} - \omega_{21} = 0.35\,\text{GHz}$

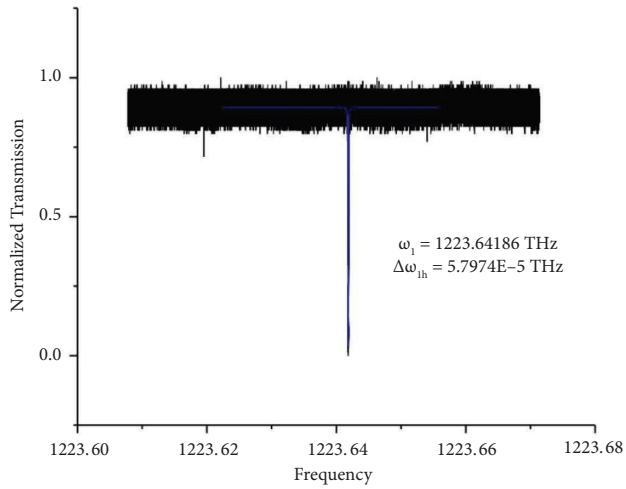

Figure 5: The frequency of microsphere cavity with no solution. There is only one original vibration modes.

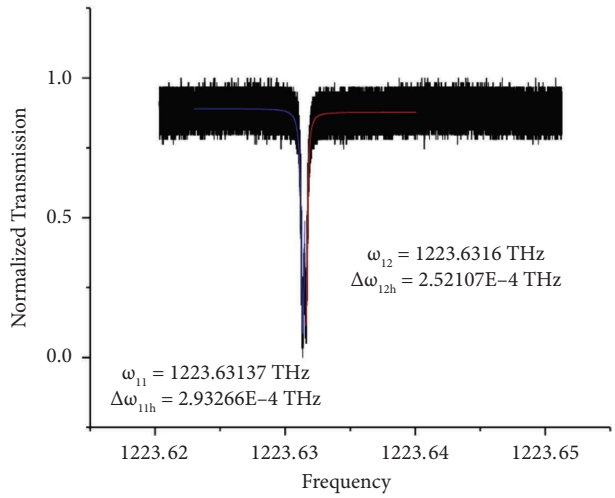

Figure 6: The frequency distribution of microsphere cavity with diluted solution. The ratio of the standard solution and the alcoholic solution is 1 : 2. The blue line and red line show that one peak splits into two frequencies.

Table 2: The result of ratio 1 : 2 (standard solution: alcoholic solution).

Original mode	$\omega_1 = 1223.64186\,\text{THz}$
Widths	$\Delta\omega_{1h} = 5.79740 \times 10^{-5}\,\text{THz}$
RDX mode	$\omega_{11} = 1223.63137\,\text{THz},\ \omega_{12} = 1223.63160\,\text{THz}$
Widths	$\Delta\omega_{11h} = 2.93266 \times 10^{-4}\,\text{THz}, \Delta\omega_{12h} = 2.52107 \times 10^{-4}\,\text{THz}$
Split frequency	$\omega_{12} - \omega_{11} = 0.23\,\text{GHz}$

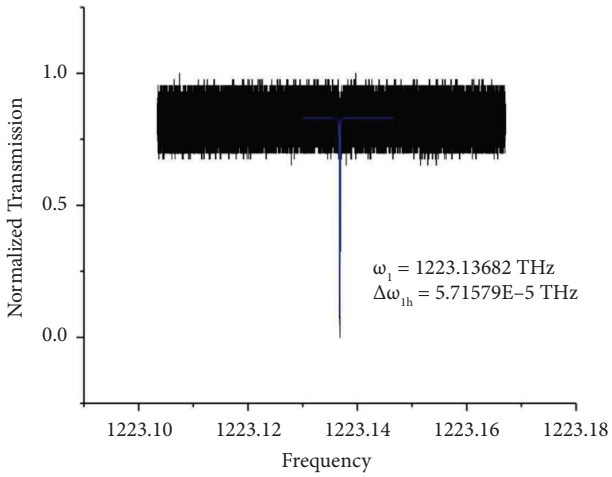

Figure 7: The original vibration mode frequency.

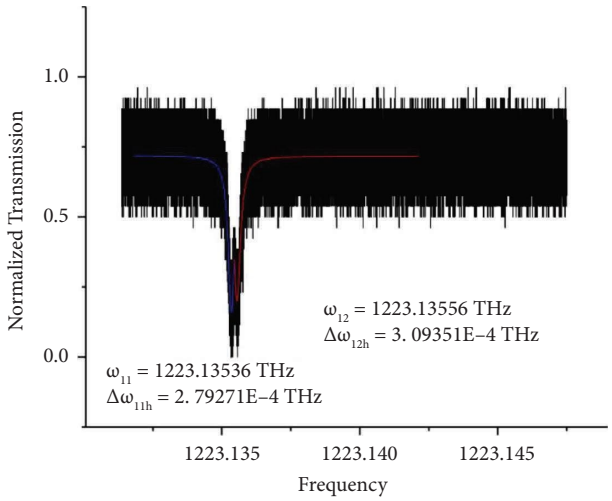

Figure 8: The ratio of the standard solution and the alcoholic solution is 1 : 3. The blue line and red line show the split frequencies.

Table 3: The result of ratio 1 : 3 (standard solution: alcoholic solution).

Original mode	$\omega_1 = 1223.13682\,\text{THz}$
Widths	$\Delta\omega_{1h} = 5.71579 \times 10^{-5}\,\text{THz}$
RDX mode	$\omega_{11} = 1223.13536\,\text{THz}, \omega_{12} = 1223.13556\,\text{THz}$
Widths	$\Delta\omega_{11h} = 2.79271 \times 10^{-4}\,\text{THz},\ \Delta\omega_{12h} = 3.09351 \times 10^{-4}\,\text{THz}$
Split frequency	$\omega_{12} - \omega_{11} = 0.20\,\text{GHz}$

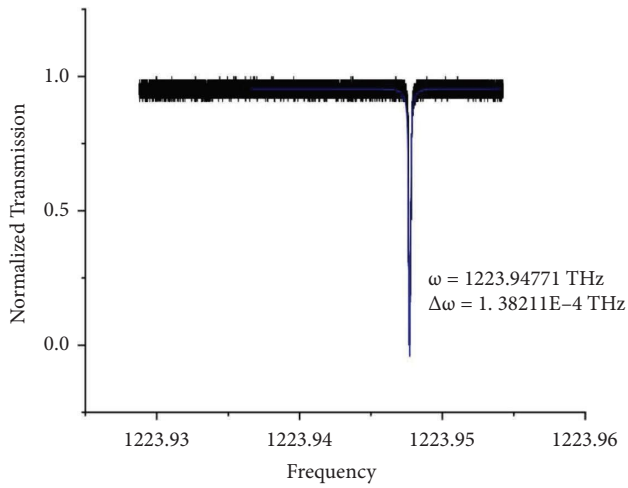

Figure 9: The frequency of original vibration mode of microsphere cavity with no solution.

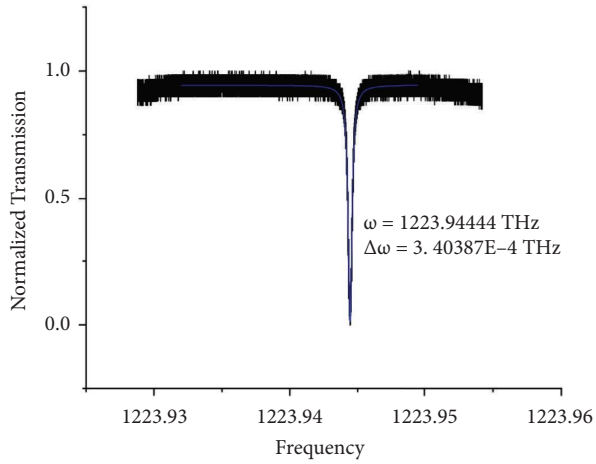

Figure 10: The frequency of pure acetone diluted by alcoholic solution with ratio 1 : 2. The vibration mode moves to another value and no split occurs.

4. Conclusion and Discussion

The optical microcavity, which is widely used in medical science [32], biology [33], and environmental science [34], is a new kind of sensor with ultrahigh sensitivity [35–37]. For example the applications include diagnosis of diseases, detection of protein of blood, the pollution of environment and so on [38–40]. We want to research the usage of optical microcavity sensor in public security field because the appearance of more and more terrorist attacks. Optical microcavity has its advantage of ultrahigh sensitivity which could reach nanoscale [30, 31]. Not only the explosive itself but also things and people that used to touch the explosive can be found using optical microcavity sensor. For example, we wipe someone's hands or clothes or something using filter papers, and then prepare the liquid or gas sample detecting in the optical microcavity sensor. The result will tell us whether someone or something touched explosive before. Because even only one nanoparticle of explosive adhere to the microcavity, it could cause the split and movement of the mode frequency peak.

In this paper, we use silica or quartz microsphere type whispering gallery mode (WGM) microcavity to show the effect of the detection of typical explosive RDX. After dipping the microsphere cavities into diluted solution, RDX molecules suspended in the solution adsorb onto the microsphere cavities and change the original vibration mode. We give three kinds of concentration as examples. The ratio of the standard solution and the alcoholic solution are 1 : 1, 1 : 2, 1 : 3. As shown in figures above, RDX molecules low, split and broaden the frequency peak obviously. When there is no RDX molecule in the standard solution which means pure acetone, the frequency peak only moves to a lower value and no split appears. The effective refraction index of the microcavity increases due to the solution, the frequency of original vibration mode shift to a lower value. According to the symmetry of the microcavity, waves in the microcavity are divided into clockwise mode and counterclockwise mode. When the molecules enter the microcavity, due to scattering, the modes of the two waves become coupled, and the frequency peak is broadened. The degeneracy due to the coupling causes the split of the frequency. The scale of the frequency split is GHz. The available concentration of diluted solution can be extremely low. The research of the detect limitations of different molecules is still processing. The noise is unavoidable in experiment. The main noises in microcavity experiment are laser wavelength drift noise, vibration of the fiber taper, quantum shot noise and the thermo refractive noise. There are several solutions to reduce the experimental noises, one can lock the vibration mode and tighten the fiber to conquer the first two noises. To reduce the quantum shot noise and thermo refractive noise, reduction of light intensity and derivation of the microcavity heat using optimization of material or configuration that has good thermal property are suggested [41]. Besides, these noises can be suppressed using the method called back-scattered light [42]. Contamination and impurity is the pretreatment of detection. The purification and extraction of chemicals is another topic. We focus on the detection process. Here, we studied RDX only one explosive to show the viability of microcavity technique and the procedure detail. We focus on the viability of technique itself in forensic science (explosive RDX as an example). It is worth noting that in this work, we only analyze the feasibility of this method, so the number of experiments is relatively small. For the later study of particle properties, a large number of experiments are needed, and the experimental data should be statistically significant. We can use this method to identify explosives. On the basis of the viability, the comparisons of different explosives and different configurations of microcavities are further works in the future.

Data Availability

The data that support the findings of this study are available on request from the corresponding author.

Conflicts of Interest

The authors declare that there are no conflicts of interest.

Authors' Contributions

Yao Shen is responsible for conceptualization, methodology, writing of the original draft, and validation. Kai Wang was responsible for experimental operation. Bai-En Guo was responsible for writing, illustration, and editing. Min Wang was responsible for validation and supervision. All authors have read and agreed to the published version of the manuscript.

Acknowledgments

The research was supported by the Fundamental Research Funds for the Central Universities (2022JKF02024), the Young Elite Scientists Sponsorship Program by the China Association for Science and Technology (2022QNRC001), and the National Natural Science Foundation of China (62131002).

References

[1] J. L. Jewell, S. L. McCall, Y. H. Lee, A. Scherer, A. C. Gossard, and J. H. English, "Lasing characteristics of GaAs microresonators," *Applied Physics Letters*, vol. 54, no. 15, pp. 1400–1402, 1989.

[2] J. M. Gérard, D. Barrier, J. Y. Marzin et al., "Quantum boxes as active probes for photonic microstructures: the pillar microcavity case," *Applied Physics Letters*, vol. 69, no. 4, pp. 449–451, 1996.

[3] O. Painter, R. K. Lee, A. Scherer et al., "Two-dimensional photonic band-gap defect mode laser," *Science*, vol. 284, no. 5421, pp. 1819–1821, 1999.

[4] G. S. Solomon, M. Pelton, and Y. Yamamoto, "Modification of spontaneous emission of a single quantum dot," *Physica Status Solidi (A)*, vol. 178, no. 1, pp. 341–344, 2000.

[5] D. K. Armani, T. J. Kippenberg, S. M. Spillane, and K. J. Vahala, "Ultra-high-Q toroid microcavity on a chip," *Nature*, vol. 421, no. 6926, pp. 925–928, 2003.

[6] C. Schneider, P. Gold, S. Reitzenstein, S. Höfling, and M. Kamp, "Quantum dot micropillar cavities with quality factors exceeding 250,000," *Applied Physics B*, vol. 122, no. 1, p. 19, 2016.

[7] P. Shapturenka, H. Stute, N. I. Zakaria, S. P. DenBaars, and M. J. Gordon, "Color-changing refractive index sensor based on Fano-resonant filtering of optical modes in a porous dielectric Fabry-Pérot microcavity," *Optics Express*, vol. 28, no. 19, pp. 28226–28233, 2020.

[8] J. Gérard, B. Sermage, B. Gayral, B. Legrand, E. Costard, and V. Thierry-Mieg, "Enhanced spontaneous emission by quantum boxes in a monolithic optical microcavity," *Physical Review Letters*, vol. 81, no. 5, pp. 1110–1113, 1998.

[9] C. J. Hood, T. W. Lynn, A. C. Doherty, A. S. Parkins, and H. J. Kimble, "The atom-cavity microscope: single atoms bound in orbit by single photons," *Science*, vol. 287, no. 5457, pp. 1447–1453, 2000.

[10] J. R. Buck and H. J. Kimble, "Optimal sizes of dielectric microspheres for cavity QED with strong coupling," *Physical Review A*, vol. 67, no. 3, Article ID 033806, 2003.

[11] K. Srinivasan, P. Barclay, O. Painter, J. Chen, C. Cho, and C. Gmachl, "Experimental demonstration of a high quality factor photonic crystal microcavity," *Applied Physics Letters*, vol. 83, p. 10, 2003.

[12] X. Y. Wu, K. Wang, H. Wang, B. Lu, Y. P. Gao, and C. Wang, "The nonlinear effects and applications of gain doped whispering-gallery mode cavities," *Europhysics Letters*, vol. 141, no. 2, Article ID 25001, 2023.

[13] B. Duan, H. Y. Zou, J. H. Chen et al., "High-precision whispering gallery microsensors with ergodic spectra empowered by machine learning," *Photonics Research*, vol. 10, pp. 2343–2348, 2022.

[14] K. Wang, H. Wang, X. Y. Wu et al., "Ultrasound sensing using packaged microsphere cavity in the underwater environment," *Sensors*, vol. 22, no. 11, p. 4190, 2022.

[15] B. Gayral, J. M. Gérard, A. Lemaître, C. Dupuis, L. Manin, and J. L. Pelouard, "High-*Q* wet-etched GaAs microdisks containing InAs quantum boxes," *Applied Physics Letters*, vol. 75, no. 13, pp. 1908–1910, 1999.

[16] R. R. Xie, G. Q. Qin, H. Zhang et al., "Phase-controlled dual-wavelength resonance in a self-coupling whispering-gallery-mode microcavity," *Optics Letters*, vol. 46, no. 4, pp. 773–776, 2021.

[17] A. S. Zolotukhina, A. O. Spiridonov, E. M. Karchevskii, and A. I. Nosich, "Electromagnetic analysis of optimal pumping of a microdisk laser with a ring electrode," *Applied Physics B*, vol. 123, no. 1, p. 32, 2017.

[18] G. Q. Qin, R. R. Xie, H. Zhang et al., "Experimental realization of sensitivity enhancement and suppression with exceptional surfaces," *Laser and Photonics Reviews*, vol. 15, 2021.

[19] K. Djordjev, S. J. Choi, P. D. Dapkus, and R. Dapkus, "Microdisk tunable resonant filters and switches," *IEEE Photonics Technology Letters*, vol. 14, no. 6, pp. 828–830, 2002.

[20] P. Rabiei, W. H. Steier, Z. Cheng, and L. R. Dalton, "Polymer micro-ring filters and modulators," *Journal of Lightwave Technology*, vol. 20, no. 11, pp. 1968–1975, 2002.

[21] D. W. Vernooy, V. S. Ilchenko, H. Mabuchi, E. W. Streed, and H. J. Kimble, "High-Q measurements of fused-silica microspheres in the near infrared," *Optics Letters*, vol. 23, no. 4, pp. 247–249, 1998.

[22] B. Peng, A. K. Ozdemir, F. Lei, F. Monifi, and Y. Lan, "Parity–time-symmetric whispering-gallery microcavities," *Nature Physics*, vol. 10, 2014.

[23] L. A. Delouise, P. M. Kou, and B. L. Miller, "Cross-correlation of optical microcavity biosensor response with immobilized enzyme activity. Insights into biosensor sensitivity," *Analytical Chemistry*, vol. 77, no. 10, pp. 3222–3230, 2005.

[24] T. Yoshie, L. Tang, and S. Y. Su, "Optical microcavity: sensing down to single molecules and atoms," *Sensors*, vol. 11, no. 2, pp. 1972–1991, 2011.

[25] K. Xin, X. F. Shi, Y. Liu, Z. M. Zhang, W. J. Jia, and J. Ma, "Method of optical manipulation of gold nanoparticles for surface-enhanced Raman scattering in a microcavity," *Optics Express*, vol. 28, no. 6, pp. 8734–8743, 2020.

[26] R. Haldar, A. Roy, P. Mondal, V. Mishra, and S. K. Varshney, "Free-carrier-driven Kerr frequency comb in optical microcavities: steady state, bistability, self-pulsation, and modulation instability," *Physical Review A*, vol. 99, no. 3, Article ID 033848, 2019.

[27] H. M. Shi, J. Y. He, H. Y. Guo, X. Q. Liu, Z. Wang, and Y. G. Liu, "Single-resonator, stable dual-longitudinal-mode optofluidic microcavity laser based on a hollow-core microstructured optical fiber," *Optics Express*, vol. 29, no. 7, pp. 10077–10088, 2021.

[28] A. Laha, D. Beniwal, and S. Ghosh, "Successive switching among four states in a gain-loss-assisted optical microcavity hosting exceptional points up to order four," *Physical Review A*, vol. 103, no. 2, Article ID 023526, 2021.

[29] C. H. Yi, H. H. Yu, and C. M. Kim, "Non-Hermitian analysis of surface creeping waves in optical microcavities: nature of external resonances," *Physical Review A*, vol. 102, no. 6, Article ID 063503, 2020.

[30] S. K. Özdemir, J. G. Zhu, X. Yang et al., "Highly sensitive detection of nanoparticles with a self-referenced and self-heterodyned whispering-gallery Raman microlaser," *Proceedings of the National Academy of Sciences*, vol. 111, 2014.

[31] G. Q. Qin, M. Wang, J. W. Wen, D. Ruan, and G. L. Long, "Brillouin cavity optomechanics sensing with enhanced dynamical backaction," *Photonics Research*, vol. 7, no. 12, pp. 1440–1446, 2019.

[32] F. Li, X. Li, X. Zhou et al., "Plug-in label-free optical fiber DNA hybridization sensor based on C-type fiber Vernier effect," *Sensors and Actuators B: Chemical*, vol. 354, Article ID 131212, 2022.

[33] J. Zhu, H. Liu, F. Bo, C. Tao, G. Zhang, and J. Xu, "Intuitive model of exceptional points in an optical whispering-gallery microcavity perturbed by nanoparticles," *Physical Review A*, vol. 101, no. 5, Article ID 053842, 2020.

[34] Y. Wang, Y. Li, Y. Li et al., "Noise canceled graphene-microcavity fiber laser sensor for ultrasensitive gas detection," *Photonics Research*, vol. 11, no. 8, p. A1, 2023.

[35] S. Barland, J. R. Tredicce, M. Brambilla et al., "Cavity solitons as pixels in semiconductor microcavities," *Nature*, vol. 419, no. 6908, pp. 699–702, 2002.

[36] A. D. Stone, "Wave-chaotic optical resonators and lasers," *Physica Scripta*, vol. 90, pp. 248–262, 2001.

[37] G. Khitrova, H. M. Gibbs, F. Jahnke, M. Kira, and S. W. Koch, "Nonlinear optics of normal-mode-coupling semiconductor microcavities," *Reviews of Modern Physics*, vol. 71, no. 5, pp. 1591–1639, 1999.

[38] W. F. Brinkman, T. L. Koch, D. V. Lang, and D. P. Wilt, "The lasers behind the communications revolution," *Bell Labs Technical Journal*, vol. 5, no. 1, pp. 150–167, 2002.

[39] L. A. Coldren, S. W. Corzine, and M. L. Mashanovitch, *Diode, Lasers and Phhotonic Integrated Circuits*, Wiley, New York, NY, USA, 1995.

[40] V. B. Taranenko and C. O. Weiss, "Spatial solitons in semiconductor microresonators," *IEEE Journal of Selected Topics in Quantum Electronics*, vol. 8, no. 3, pp. 488–496, 2002.

[41] X. F. Jiang, M. Wang, M. C. Kuzyk, T. Oo, G. L. Long, and H. L. Wang, "Chip-based silica microspheres for cavity optomechanics," *Optics Express*, vol. 23, no. 21, pp. 27260–27265, 2015.

[42] J. Knittel, J. Swaim, D. McAuslan, G. A. Brawley, and W. P. Bowen, "Back-scatter based whispering gallery mode sensing," *Scientific Reports*, vol. 3, no. 1, p. 2974, 2013.